Journal of Nuclear Medicine, published on February 14, 2020 as doi:10.2967/jnumed.119.238105

Performance of digital PET compared to high-resolution conventional PET in patients with cancer

Daniëlle Koopman[1,2], Jorn. A. van Dalen[3], Henk Stevens[1], Cornelis H. Slump[2], Siert Knollema[1] and Pieter L. Jager[1]

Department of Nuclear Medicine[1] and Medical Physics[3], Isala, Zwolle, The Netherlands

Technical Medicine Centre[2], University of Twente, Enschede, The Netherlands

Correspondence:

Daniëlle Koopman, PhD in Technical Medicine

Dokter van Heesweg 2, 8025 AB Zwolle, The Netherlands

+31 38 424 5238

ORCID 0000-0002-8976-5434

Word count: 4982

Running title: dPET performance in patients with cancer

ABSTRACT

Recently introduced PET systems using silicon photomultipliers with digital readout (dPET) have an improved timing and spatial resolution, aiming at a better image quality, over conventional PET (cPET) systems. We prospectively evaluated the performance of a dPET system in patients with cancer, as compared to high-resolution (HR) cPET imaging.

Methods:

After a single FDG-injection, 66 patients underwent dPET (Vereos, Philips Healthcare) and cPET (Ingenuity TF, Philips Healthcare) imaging in a randomized order. We used HR-reconstructions (2x2x2 mm^3 voxels) for both scanners and determined SUV_{max}, SUV_{mean}, lesion-to-background ratio (LBR), metabolic tumor volume (MTV) and lesion diameter in up to 5 FDG-positive lesions per patient. Furthermore, we counted the number of visible and measurable lesions on each PET scan. Two nuclear medicine specialists blindly determined the Tumor Node Metastasis (TNM) score from both image sets in 30 patients referred for initial staging. For all 66 patients, these specialists separately and blindly evaluated image quality (4-point scale) and determined the scan preference.

Results

We included 238 lesions that were visible and measurable on both PET scans. We found 37 additional lesions on dPET in 27 patients (41%), which were unmeasurable (n=14) or invisible (n=23) on cPET. SUV_{mean}, SUV_{max}, LBR and MTV on cPET were 5.2±3.9 (mean±SD), 6.9±5.6, 5.0±3.6 and 2991±13251 mm^3, respectively. On dPET SUV_{mean}, SUV_{max} and LBR increased 24%, 23% and 27%, respectively ($p<0.001$) while MTV decreased 13% ($p<0.001$) compared to cPET. Visual analysis showed TNM upstaging with dPET in 13% of the patients (4/30). dPET images also scored higher in image quality ($p=0.003$) and were visually preferred in the majority of cases (65%).

Conclusion

Digital PET improved the detection of small lesions, upstaged the disease and images were visually preferred as compared to high-resolution conventional PET. More studies are necessary to confirm the superior diagnostic performance of digital PET.

Keywords

Digital PET; Conventional PET; FDG-PET; lesion detection; cancer imaging

INTRODUCTION

Positron Emission Tomography (PET) combined with Computed Tomography (CT), using fluor-18 fluordeoxyglucose (FDG), is increasingly important for cancer management *(1,2)*. However, two major limitations of PET scanners are the limited system sensitivity, resulting in a low signal-to-noise ratio and the low spatial resolution *(3),* which introduces the partial volume effect (PVE) *(4)*. This PVE hampers the detection of small lesions (<20 mm) because they appear blurred in the PET image, resulting in an underestimation of lesion FDG-uptake combined with an overestimation of lesion size *(5)*.

A recent development in PET technology is the introduction of silicon photomultipliers (SiPM) with digital readout *(6)*, replacing the conventional photomultipliers. It has been shown that PET systems with digital SiPMs have an improved spatial and timing resolution, potentially resulting in a better image quality with higher standardized uptake values (SUVs) compared to conventional PET (cPET) systems *(6-8)*.

Previous studies compared cPET and dPET scans in patients with cancer using a prototype dPET *(9)* and clinically available dPET systems *(10-12)*. In general, these studies compared dPET using high-resolution (HR) reconstructions with cPET using standard-resolution (SR) reconstructions. It has been shown that moving from SR to HR reconstructions in cPET scans, e.g. by using smaller voxels, significantly improves image quality and already results in typically 25% higher SUVs and signal-to-noise ratios *(13,14)*. It is unclear which part of the previously reported improvements was the result of the dPET system and which part was due to the difference in image reconstruction *(15)*. Therefore, we prospectively evaluated the performance of a dPET scanner as compared to a cPET scanner in patients with various types of cancer, now using HR reconstructions for both systems. We performed semi-quantitative and visual assessments and investigated the effect of dPET on lesion detection capabilities as well as the impact on the Tumor Node Metastasis (TNM) disease stage.

MATERIAL AND METHODS

Patient Population

We prospectively included 66 patients with proven cancer who were referred for whole-body FDG-PET/CT for disease staging or restaging purposes, as part of an ongoing prospective single-center side-by-side PET comparison study. The Medical Ethical Committee of our institute approved the study protocol (NL52329.075.15) and the study was registered at clinicaltrials.gov with identifier #NCT03457506. Written informed consent was obtained from all participants included in this study.

PET/CT Acquisition

Patients fasted for at least 6h prior to the start of the first PET scan. Patients were administered an FDG-activity based on $A = 6.2\,w^2/t$, where A is the administered activity (in MBq), w the patient's body weight (in kg) and t the acquisition time per bed position (in s).

For each patient whole-body PET/CT scans from head to groin were acquired in supine position using a state-of-the-art time-of-flight (TOF) PET/CT scanner with conventional photomultiplier technology (cPET, Ingenuity TF, Philips Healthcare) and a TOF-PET/CT scanner with digital SiPMs (dPET, Vereos, Philips Healthcare). PET system specifications can be found elsewhere *(4)*. The PET scanning order was randomized per patient. 27 patients were first scanned on dPET followed by cPET (*dPET-first*) and 39 patients were first scanned on cPET and then on dPET (*dPET-second*). Per patient, we collected ΔT_{cPET} and ΔT_{dPET}, defined as the time between FDG-administration and start of the cPET scan and dPET scan, respectively.

PET acquisition times of the first scan were 72 s and 144 s per bed position for patients with body weight ≤80 kg and >80 kg, respectively. For the second scan, we used the acquisition time of the first scan plus a compensation for fluor-18 decay between the two scans. The average administered FDG-activity was 397 MBq (range 212-660 MBq). Prior to each PET scan, a CT scan was acquired for attenuation correction. The CT scan parameters were 120 kV, 64 mAs (average across patients), 64×0.625 mm slice collimation, a pitch of 0.83 and a rotation time of 0.5 s.

PET Reconstruction

For cPET, we applied an Ordered Subset Expectation Maximization TOF-PET HR reconstruction with 2x2x2 mm^3 voxels, a relaxation parameter of 0.6, 3 iterations and 43 subsets, without point-spread-function modelling. For

dPET, we performed an Ordered Subset Expectation Maximization TOF-PET HR reconstruction with 2x2x2 mm^3 voxels, 3 iterations and 17 subsets, without post-smoothing or point-spread-function modelling, as previously described *(16)*. These settings led to similar noise properties in cPET and dPET images for a fixed dose and scan-time per bed position, as we concluded from background measurements in a NEMA image quality phantom filled with FDG (data not shown).

Semi-quantitative Evaluation

We performed background measurements in the reconstructed PET images by drawing two regions-of-interest (ROIs) of 1000 mm^2 in three axial slices containing healthy liver tissue. The average noise level in the liver was determined as the ratio between the standard deviation (SD) and the average SUV (SUV_{liver}).

We also evaluated lesion detection capabilities for both PET scanners. An experienced PET reader counted the number of lesions with increased FDG-uptake on both PET scans in a blinded-fashion. Thereby, we gathered all lesions that were unmeasurable or invisible on one of both PET scans as follows. A lesion was regarded *unmeasurable* if it was not possible to define a 70% isocontour volume-of-interest (VOI) based on the maximum pixel value without contaminating the lesion VOI with background tissue. This can occur when there is a relatively low lesion-to-background contrast and/or heterogeneous uptake of FDG *(17)*. Furthermore, a lesion was regarded *invisible* if it was visible on only one of the PET scans.

For each patient a maximum of 5 FDG-positive lesions were included in the semi-quantitative evaluation to prevent bias from patients with many lesions. In case a patient had more than 5 eligible lesions, we selected the 5 lesions with the smallest diameter on the CT scan that were measurable on both PET scans. For all measurable lesions on both scans, a VOI was drawn around the lesion and thresholding was applied at 70% of the maximum pixel value, using IntelliSpace Portal (Version 9, Philips Healthcare) *(17)*. From the resulting volume, we measured the mean and maximum standardized uptake value (SUV_{mean} and SUV_{max}) and the metabolic tumor volume (MTV) in mm^3. Moreover, we calculated the lesion-to-background ratio (LBR) by dividing lesion's SUV_{max} to the SUV_{mean} in the background (SUV_{bkg}) directly surrounding the lesion, using the method that we described previously *(14)*. Finally, we collected the size of each lesion by measuring the short-axis diameter on the axial CT slice.

TNM Scoring

Two experienced nuclear medicine (NM) specialists who were blinded to scanner type, together determined the TNM score on both image sets of 30 patients who were referred for initial disease staging, excluding the 5 patients with initial staging for lymphoma. Next, TNM score differences between both scans were collected per patient. We used the latest published version of the TNM system for each type of cancer, as available in August 2019.

Visual Analysis and Preferences

Both NM specialists separately compared both PET scans side-by-side, blinded to scanner type. With a 4-point score, they rated the image quality of each PET scan as *1: poor, 2: moderate, 3: good* or *4: excellent* and the diagnostic confidence per scan as *1: uncertain, 2: moderate certainty, 3: good certainty* or *4: high certainty.* Furthermore, they determined their preference (*scan 1, scan 2* or *no preference*) for all 66 patients, again blinded to scanner type. In discrepant cases between both NM specialists, a third expert reader performed an additional read.

Statistical Analysis

Semi-quantitative data are presented as mean ± standard deviation (SD). Data distribution normality was evaluated using the Shapiro-Wilk test. For data that were not normally distributed, the median is included as well. We performed an independent-samples t-test to compare patient and scan characteristics (age, body weight, administered FDG-activity, ΔT and lesion size) between patients in both scanning groups. The average SUV_{mean}, SUV_{max}, LBR and MTV as measured on cPET and dPET were compared using the Wilcoxon signed-rank test. The noise in the liver as measured with both scanners was compared using a paired-samples t-test. Furthermore, for all semi-quantitative lesion-parameters (SUV_{mean}, SUV_{max}, LBR and MTV) we calculated the relative difference Δx between cPET and dPET using **Formula 1**:

$$\Delta x = (value\ dPET - value\ cPET)/value\ cPET \qquad (1)$$

We used the independent-samples Mann-Whitney U test to compare Δx between lesions in the dPET-first group and the dPET-second group. Furthermore, we performed the F-test and calculated Pearson correlation coefficients between ΔT_{dPET} and Δx, respectively. Finally, a chi-square test was performed to compare image quality and diagnostic confidence scores between cPET and dPET. A p-value less than 0.05 was considered to indicate statistical significance.

RESULTS

Patient and scan characteristics are shown in **Table 1**. We included 238 FDG-positive lesions with an average size of 12±12 mm (median 9 mm, range 4-90 mm) in 66 patients. The average lesion size was similar in both scanning groups with 12±9 mm in the dPET-first group and 13±13 mm in the dPET-second group (p=0.80).

Lesion Detection Capabilities

In 27 out of 66 patients (41%) we found 37 additional FDG-positive lesions on the dPET images, that were unmeasurable (n=14) or invisible (n=23) on the cPET images. Eight of these lesions were detected when dPET was performed first (4 unmeasurable, 4 invisible). The remaining 28 lesions (10 unmeasurable, 19 invisible) appeared on the dPET-second scan, i.e. after prolonged FDG-uptake time. No additional lesions were found on cPET images.

Semi-quantitative Results

The average SUV_{mean}, SUV_{max}, LBR and MTV across 238 lesions as measured on cPET and dPET images are shown in **Table 2**. With dPET we found average increases of 24%, 23% and 27% in SUV_{mean}, SUV_{max} and LBR compared to cPET, respectively (p<0.001), while the average MTV decreased with 13% on dPET. This decrease in MTV is also visible in **Figure 1,** showing a histogram with the number of lesions in MTV-subgroups as measured on cPET and dPET. With MTV measurements performed on dPET, there were more lesions with a volume smaller than 200 mm^3.

The image noise in the liver was slightly higher on dPET (14.7%±1.9%) compared to cPET (13.3%±1.8%) (p<0.001).

The relative difference per lesion-parameter between cPET and dPET is presented in **Table 3** for both scanning groups. ΔSUV_{mean}, ΔSUV_{max} and ΔLBR were significantly higher for lesions in the dPET-second group as compared to lesions in the dPET-first group (p<0.001) while ΔMTV was similar in both scanning groups (p=0.18). In particular, in the dPET-first group we found an average increase of 9% for both ΔSUV_{mean} and ΔSUV_{max} on dPET while for lesions in the dPET-second group we found average increases of 35% and 34% on dPET, respectively.

In **Figure 2**, the relative change from cPET to dPET for all lesion-parameters is compared with ΔT_{dPET} across all lesions. It shows that ΔSUV_{mean}, ΔSUV_{max} and ΔLBR further increased at prolonged ΔT_{dPET} ($p<0.001$) with correlation coefficients of 0.53, 0.52 and 0.50, respectively. ΔMTV was not correlated with ΔT_{dPET} ($p=0.14$, correlation coefficient -0.09).

TNM Staging

We found TNM upstaging with dPET in 4/30 patients (13%). Clinical information about these four cases is presented in **Table 4**. In three of these cases this dPET scan was acquired after the cPET scan (*dPET-second group*). No TNM upstaging was found with cPET.

FDG-PET images from a patient with breast cancer with TNM upstaging on dPET are shown in **Figure 3**. The TNM score on the cPET scan was T4N0M0 but the dPET scan showed a FDG-positive internal mammary lymph node (SUV_{mean} 3.2, SUV_{max} 4.0, MTV 264 mm^3) that was not visible on cPET, revealing N3 disease. After surgery, pathology findings confirmed that this lymph node was malignant.

Visual Analysis and Preferences

dPET resulted in better image quality scores compared to cPET ($p=0.003$) while the diagnostic certainty of both scans was comparable ($p=0.69$) (**Figure 4**). The majority of all PET scans resulted in a ‘good’ image quality (94% for cPET, 83% for dPET) while 15% of the dPET scans were regarded to have an ‘excellent’ image quality. The remaining 6% (cPET) and 2% (dPET) of the scans were scored as ‘moderate’ image quality.

The dPET scan was preferred in 65% of the cases, while the remaining 35% included both cPET scan preferences (11%) and no preferences (24%) (**Figure 5**). Furthermore, the scan acquired after prolonged FDG-uptake (scan 2) was preferred in 61% of the cases while the first scan was preferred in only 15% of the cases. In the dPET-second group, the dPET scan was preferred in 85% of the cases while in the dPET-first subgroup the preferences scores were more widely distributed with 37% preference for scan 1 (being dPET), 26% preference for scan 2 (being cPET) and 37% of the scans with no preference.

DISCUSSION

We performed the first prospective study that compared HR cPET with HR dPET in a relatively large cohort of 66 patients. With dPET we observed significantly higher semi-quantitative values as compared to cPET. Furthermore,

in 27 out of 66 patients (41%) we found additional lesions on dPET and in 4 patients (13%) we observed TNM upstaging on dPET. Moreover, dPET images provided a better image quality and were visually preferred by the NM specialists.

This study shows that dPET provides an improved lesion detection capability. We detected 37 additional lesions with dPET that were unmeasurable or invisible on cPET images. Most of these lesions (78%) were found on the dPET scan that was acquired *after* the cPET scan, thus with prolonged FDG-uptake time, albeit we also detected 8 additional lesions (22%) on the dPET scan that was acquired *prior to* the cPET scan. We did not found additional lesions on cPET. At least three other studies previously observed additional lesions on dPET as compared to cPET. Nguyen et al.*(9)* reported 8 additional lesions in 21 patients while Baratto et al. *(10)* found 37 additional lesions with focal FDG uptake in 50 patients. However, in these studies all dPET scans were acquired *after* the cPET acquisition, which may introduce a bias due to prolonged FDG-uptake *(18)*. Another study by López-Mora et al. *(12)* reported 22 additional small (<10 mm) lesions on dPET images in 100 patients. However, they compared SR cPET with HR dPET and did not describe whether the additional lesions were detected on the dPET-first or dPET-second scan.

Our semi-quantitative analysis showed average increases of 24% (SUV_{mean}), 23% (SUV_{max}) and 27% (LBR) across 238 FDG-positive lesions when using HR dPET instead of HR cPET. The corresponding standard deviations of 23%, 24% and 33% demonstrate that there was a wide distribution in relative changes between lesions (**Figure 2**). This variation is partly caused by methodological aspects such as the impact of prolonged FDG-uptake time *(18)* and test-retest variations *(19,20)* between two PET scans.

Nevertheless, the average semi-quantitative increases with dPET in our study were lower than findings from earlier cPET-dPET comparisons. For example, Baratto et al. *(10)* reported an average SUV increase of 53% with dPET across 107 lesions. This increase is more than twice as high as the ΔSUV in our study. This can partly be explained by the difference in scanning order because in their study all dPET scans were acquired *after* the cPET scans and this could result in ΔSUV overestimations assigned to the dPET system *(18)*. Moreover, there were also some differences between their cPET and dPET reconstruction protocol which may further cause their larger SUV difference between both PET systems. Another study by Fuentes-Ocampo et al. *(11)* recently reported an average SUV increase of 35% across 87 lesions in 87 oncological patients but they compared SR cPET with HR dPET. This difference in reconstruction approach makes their comparison invalid *(15)*. As we previously

demonstrated, the use of a HR cPET reconstruction already results in SUV increases of typically 25% as compared to SR cPET *(13,14)*.

Furthermore, we observed a 13% decrease in lesion-MTV with dPET, using 70% SUV_{max} thresholds. Nguyen et al. *(9)* also compared tumor volumes of 24 lesions on cPET and dPET. Using 35% and 50% SUV_{max} thresholds for delineation, they reported tumor volume decreases of 31% and 19%, respectively. These decreases in MTV are likely caused by the higher resolution of the dPET system that decreases the PVE.

The impact of prolonged FDG-uptake time is significant, which makes PET system comparisons after a single FDG injection difficult. Between the two scanning groups in our study, we observed significant differences in ΔSUV_{mean}, ΔSUV_{max} and ΔLBR. For example, the average ΔSUV_{mean} in the dPET-first group was only 9% whereas the average ΔSUV_{mean} in dPET-second group was 35%. Based on these averages, we expect that about (35%-9%)/2=13% of the higher SUVs on the second scan can be attributed to the prolonged scan time, which was on average 32 minutes in our study. For certain tumor types, these time-dependent SUV increases can be even higher *(18,21)*. Overall, this demonstrates that in FDG-PET comparison studies where the scan on the newer system is always acquired *after* the scan on the older system *(9,10,22)*, an overestimation of the added value of the newer PET system is likely.

The present study has some limitations. Our randomization led to 27 patients with dPET-first and 39 patients with dPET-second, which is not perfectly balanced. This may cause slight SUV overestimation, although we demonstrated that general patient characteristics and lesion sizes between both groups were similar. Moreover, we aimed to perform a comparison of cPET and dPET using HR reconstructions for small lesion detection in order to solely determine the impact of new dPET technology. However, the image reconstructions were not exactly similar, as we did not have the same software possibilities available on the two different scanners. To minimize the impact of these differences, we selected reconstruction settings that led to similar noise levels in phantom images. Another limitation of our study is that we did not evaluate the diagnostic performance of dPET in terms of sensitivity, specificity and accuracy due to limited verification data. Further studies are required for this purpose.

CONCLUSION

In this prospective head-to-head evaluation, digital PET improved the detection of small lesions over high-resolution conventional PET. Digital PET scans were visually preferred by experienced readers, additional lesions were detected in 41% of the patients and the disease was upstaged in 13%. More studies are necessary to confirm the superior diagnostic performance of digital PET.

ACKNOWLEDGEMENTS

We gratefully acknowledge Tessa Gerritse and Ellis Simons-Winters for their assistance in patient inclusion and we thank the staff from Isala, Zwolle and the Technical Medicine Centre, University of Twente, Enschede for their overall support and kind collaboration.

The Department of Nuclear Medicine, Isala, has established a research cooperation with Philips Healthcare regarding new PET technologies. The content of the article was solely the responsibility of the authors. No other potential conflicts of interest relevant to this article were reported.

KEY POINTS

Question: What is the performance of a digital PET system, in terms of lesion detection, image quality and disease staging, in patients with cancer as compared to high-resolution conventional PET imaging?

Pertinent Findings: We performed a prospective head-to-head FDG-PET comparison study in 66 patients with proven cancer using conventional PET (Ingenuity TF, Philips) and digital PET (Vereos, Philips) and with HR reconstructions on both systems. With digital PET we found 37 additional lesions in 27 patients (41%), 25% increase in lesion-SUVs and TNM upstaging in 13% of the patients. Furthermore, digital PET images showed an improved quality and were visually preferred in the majority of cases (65%).

Implications for Patient Care: With improved small lesion detection and upstaging in some cases, digital PET may provide a more accurate diagnosis compared to conventional PET and this could influence patient treatment and prognosis.

REFERENCES

1. Bar-Shalom R, Yefremov N, Guralnik L, et al. Clinical performance of PET/CT in evaluation of cancer: Additional value for diagnostic imaging and patient management. *J Nucl Med*. 2003;44:1200-1209.

2. Branstetter IV BF, Blodgett TM, Zimmer LA, et al. Head and neck malignancy: Is PET/CT more accurate than PET or CT alone? *Radiology*. 2005;235:580-586.

3. Takamochi K, Yoshida J, Murakami K, et al. Pitfalls in lymph node staging with positron emission tomography in non-small cell lung cancer patients. *Lung Cancer*. 2005;47:235-242.

4. van der Vos C, Koopman D, Rijnsdorp S, et al. Quantification, improvement, and harmonization of small lesion detection with state-of-the-art PET. *Eur J Nucl Med Mol Imaging*. 2017;44:4-16.

5. Soret M, Bacharach SL, Buvat I. Partial-volume effect in PET tumor imaging. *J Nucl Med*. 2007;48:932-945.

6. Rausch I, Ruiz A, Valverde-Pascual I, Cal-González J, Beyer T, Carrio I. Performance evaluation of the vereos PET/CT system according to the NEMA NU2-2012 standard. *J Nucl Med*. 2019;60:561-567.

7. Hsu DF, Ilan E, Peterson WT, Uribe J, Lubberink M, Levin CS. Studies of a next-generation silicon-photomultiplier–based time-of-flight PET/CT system. *J Nucl Med*. 2017;58:1511-1518.

8. van Sluis JJ, de Jong J, Schaar J, et al. Performance characteristics of the digital biograph vision PET/CT system. *J Nucl Med*. 2019;60:1031-1036.

9. Nguyen NC, Vercher-Conejero J, Sattar A, et al. Image quality and diagnostic performance of a digital PET prototype in patients with oncologic diseases: Initial experience and comparison with analog PET. *J Nucl Med*. 2015;56:1378-1385.

10. Baratto L, Park SY, Hatami N, et al. 18F-FDG silicon photomultiplier PET/CT: A pilot study comparing semi-quantitative measurements with standard PET/CT. *PloS one*. 2017;12:e0178936.

11. Fuentes-Ocampo F, López-Mora DA, Flotats A, et al. Digital vs. analog PET/CT: Intra-subject comparison of the SUVmax in target lesions and reference regions. *Eur J Nucl Med Mol Imaging*. 2019;46:1745-1750.

12. López-Mora DA, Flotats A, Fuentes-Ocampo F, et al. Comparison of image quality and lesion detection between digital and analog PET/CT. *Eur J Nucl Med Mol Imaging*. 2019;46:1383-1390.

13. Koopman D, van Dalen JA, Lagerweij MCM, et al. Improving the detection of small lesions using a state-of-the-art time-of-flight PET/CT system and small-voxel reconstructions. *J Nucl Med Technol*. 2015;43:21-27.

14. Koopman D, van Dalen JA, Arkies H, et al. Diagnostic implications of a small-voxel reconstruction for loco-regional lymph node characterization in breast cancer patients using FDG-PET/CT. *EJNMMI Res*. 2018;8:3-12.

15. Koopman D, Jager PL, van Dalen JA. Small-voxel reconstructions significantly influence SUVs in PET imaging. *Eur J Nucl Med Mol Imaging*. 2019;46:1751-1752.

16. Koopman D, Koerkamp MG, Jager PL, et al. Digital PET compliance to EARL accreditation specifications. *EJNMMI Phys*. 2017;4:9-14.

17. Velasquez LM, Boellaard R, Kollia G, et al. Repeatability of 18F-FDG PET in a multicenter phase I study of patients with advanced gastrointestinal malignancies. *J Nucl Med*. 2009;50:1646-1654.

18. Lowe VJ, DeLong DM, Hoffman JM, Coleman RE. Optimum scanning protocol for FDG-PET evaluation of pulmonary malignancy. *J Nucl Med*. 1995;36:883-887.

19. de Langen AJ, Vincent A, Velasquez LM, et al. Repeatability of 18F-FDG uptake measurements in tumors: A metaanalysis. *J Nucl Med*. 2012;53:701.

20. Kramer GM, Frings V, Hoetjes N, et al. Repeatability of quantitative whole-body 18F-FDG PET/CT uptake measures as function of uptake interval and lesion selection in non–small cell lung cancer patients. *J Nucl Med*. 2016;57:1343-1349.

21. Shankar LK, Hoffman JM, Bacharach S, et al. Consensus recommendations for the use of 18F-FDG PET as an indicator of therapeutic response in patients in national cancer institute trials. *J Nucl Med*. 2006;47:1059-1066.

22. Sonni I, Park S, Baratto L, et al. Initial experience with a SiPM-based PET/CT scanner: Influence of acquisition time on image quality. *J Nucl Med*. 2017;58 (supplement 1):1369.

FIGURES

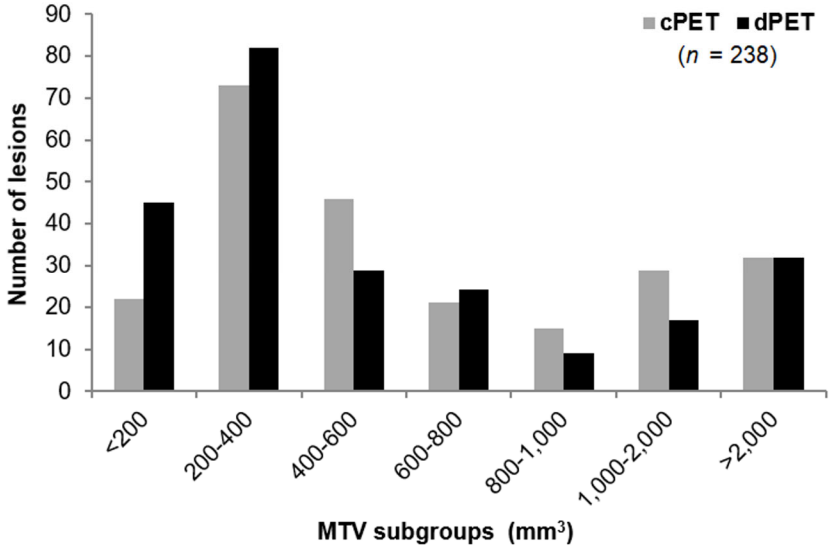

FIGURE 1 Histogram showing the decrease in MTV on dPET images as compared to cPET, especially for lesions <200 mm^3

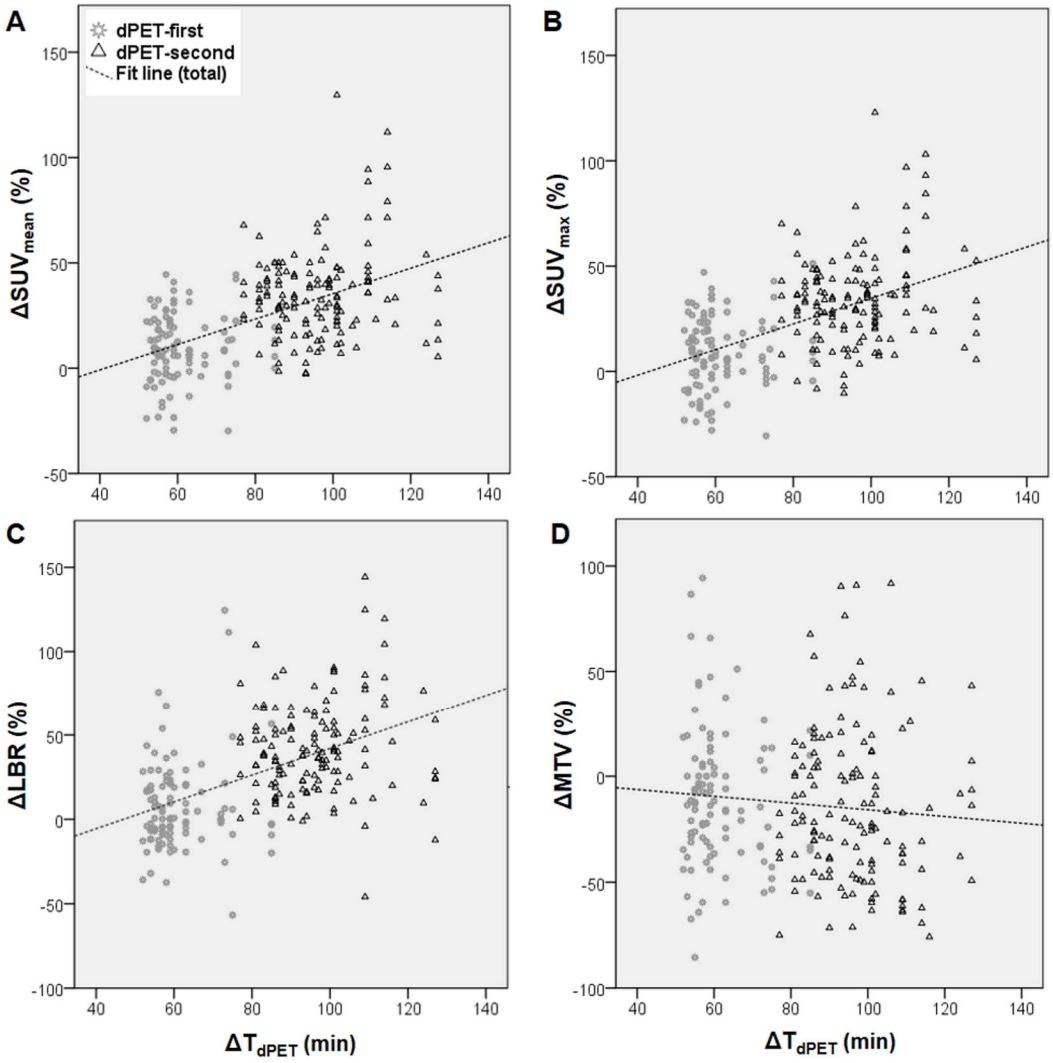

FIGURE 2 Scatter plots comparing ΔSUV_{mean} (A), ΔSUV_{max} (B), ΔLBR (C) and ΔMTV (D) with ΔT_{dPET} for lesions in the dPET-first and dPET-second group. The relative change in SUV_{mean}, SUV_{max} and LBR increased with prolonged ΔT_{dPET} ($p<0.001$) while we found no correlation between ΔMTV and ΔT_{dPET} ($p=0.14$)

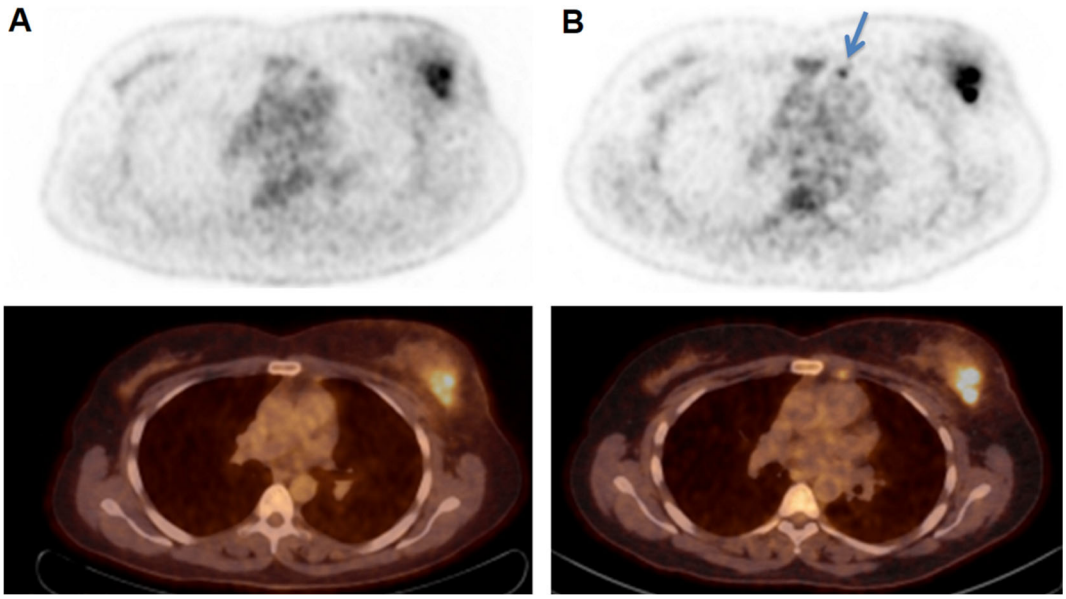

FIGURE 3 FDG-PET/CT images from a patient with breast cancer with upstaging from T4N0M0 on cPET (ΔT=54 min) (A) to T4N3M0 on dPET (ΔT=106 min) (B). dPET images revealed a FDG-positive internal mammary lymph node (blue arrow) with a diameter of 7 mm. During surgery, a sentinel node procedure was performed and it was confirmed by pathology that this lymph node was malignant

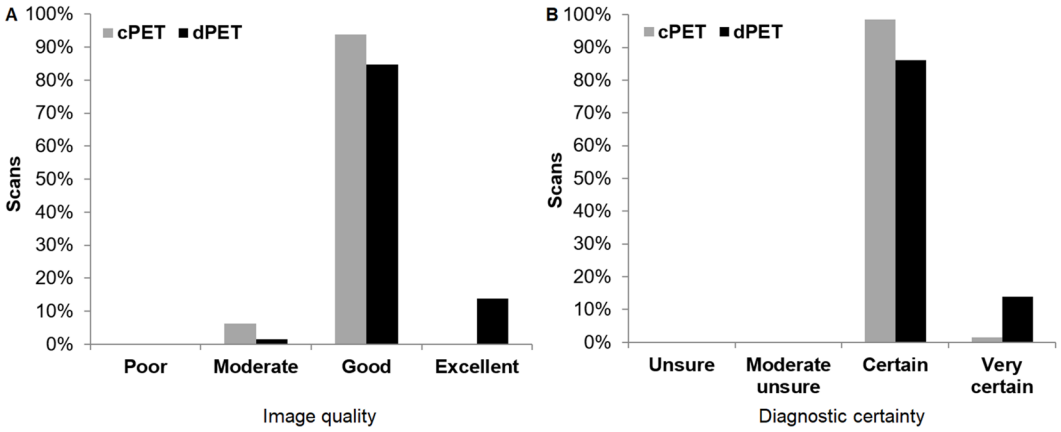

FIGURE 4 Bar plots showing image quality (A) and diagnostic certainty scores (B) of cPET and dPET scans. Higher image quality scores were found for dPET scans (p=0.003) while the diagnostic certainty was comparable between cPET and dPET scans (p=0.68)

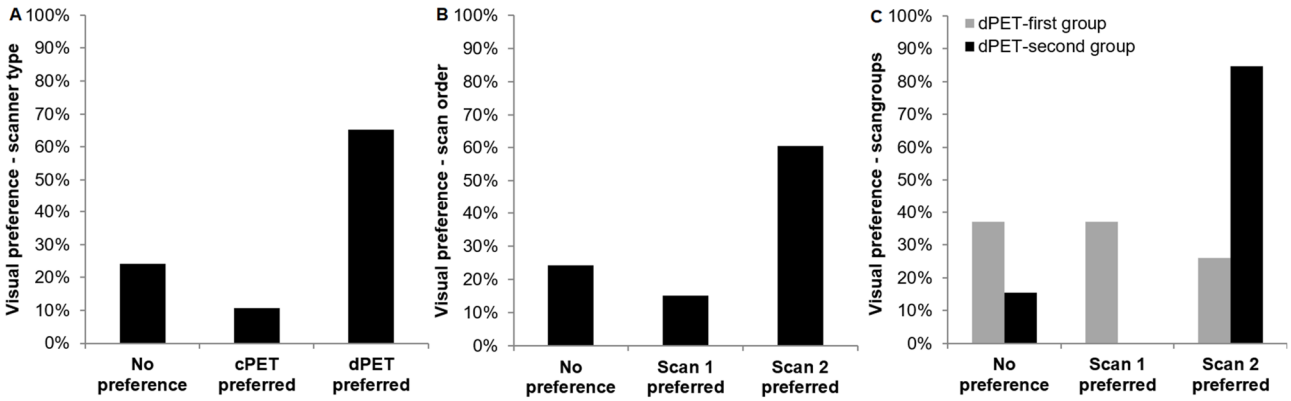

FIGURE 5 Bar plots showing scanner type preferences (A), scan order preferences (B) and scan order preferences per scanning group (C). Overall, the dPET scan as well as the second scan were preferred in the majority of the cases (65% and 61%, respectively). Moreover, the dPET scan was preferred in 85% of the cases when it was acquired after the cPET scan

TABLES

TABLE 1 Patient and scan characteristics

	dPET-first group (n=27)	dPET-second group (n=39)	*p-value*
Gender (n)			
Male	15	23	
Female	12	16	
Age (in years)*	65 ± 11	70 ± 17	*0.19*
Cancer type			
Lung cancer	17	22	
Breast cancer	7	3	
Esophageal cancer	0	8	
Other	3	6	
PET scan indication			
Initial disease staging	14	21	
Restaging or follow up	13	18	
Body weight (in kg)*	84 ± 19	78 ± 15	*0.14*
Administered FDG-activity (in MBq)*	393 ± 111	400 ± 93	*0.77*
ΔT			
until first PET scan (in min)*	62 ± 9	65 ± 10	*0.18*
until second PET scan (in min)*	95 ± 12	97 ± 12	*0.48*

* Continuous variables are described as mean ± SD

† PET: Positron Emission Tomography. FDG: Fluor-18 Fluordeoxyglucose. SD: Standard Deviation. cPET: conventional PET. dPET: digital PET.

TABLE 2 Semi-quantitative values as measured on both scanners across all lesions (n=238) and relative differences between cPET and dPET. SUV_{mean}, SUV_{max} and LBR were typically 25% higher on dPET ($p<0.001$), while the MTV (in mm^3) was on average 13% lower on dPET ($p<0.001$)

		SUV_{mean}	**SUV_{max}**	**LBR**	**MTV (in mm^3)**
cPET	**Mean ± SD**	5.2 ± 3.9	6.9 ± 5.6	5.0 ± 3.6	2991 ± 13251
	Median	3.8	4.9	3.8	492
dPET	**Mean ± SD**	6.2 ± 4.4	8.3 ± 6.7	6.1 ± 4.1	2692 ± 10219
	Median	4.7	6.0	4.9	360
Relative difference Δx (%)		24% ± 23%	23% ± 24%	27% ± 33%	-13% ± 35%

* PET: Positron Emission Tomography. SUV: Standardized Uptake Value. LBR: Lesion-to-Background Ratio. MTV: Metabolic Tumour Volume. SD: Standard Deviation

TABLE 3 Relative differences in semi-quantitative parameters between cPET and dPET per scanning group. ΔSUV_{mean}, ΔSUV_{max} and ΔLBR were significantly higher for lesions included in the dPET-second group compared to the dPET-first group, indicating that the scanning order and FDG-uptake time have significant impact on relative differences between cPET and dPET for these parameters. ΔMTV was similar across both groups

	dPET-first (n=101)	**dPET-second (n=137)**	**p-value**
ΔSUV_{mean} *	9% ± 17%	35% ± 21%	<0.001
ΔSUV_{max} *	9% ± 17%	34% ± 22%	<0.001
ΔLBR *	7% ± 27%	42% ± 28%	<0.001
ΔMTV *	-10% ± 33%	-15% ± 37%	0.18

* Continuous variables are described as mean ± SD

† PET: Positron Emission Tomography. cPET: conventional PET. dPET: digital PET. SUV: Standardized Uptake Value. LBR: Lesion-to-Background Ratio. FDG: Fluor-18 Fluordeoxyglucose. MTV: Metabolic Tumour Volume. SD: Standard Deviation

TABLE 4 Description of four patients with TNM upstaging on dPET

Pt	Diagnosis	Scanning group	TNM stage on cPET	TNM stage on dPET	Additional information
1	Breast cancer	dPET-second	T4N0M0	T4N3M0	Suspected internal mammary lymph node metastasis. Confirmed by pathology results.
2	Lung cancer	dPET-first	T4N3M1a	T4N3M1b	Suspected right adrenal gland metastasis on dPET. No validation information available.
3	Lung cancer	dPET-second	T1aN2M0	T1aN3M0	Suspected lymph node metastasis near the thyroid gland. Further SUV rise on follow-up FDG-PET scans after 6 and 12 months.
4	Esophageal cancer	dPET-second	T1N0M0	T1N0M1	Suspected FDG-positive lesion in the right pelvis region. No validation information available.

* PET: Positron Emission Tomography. TNM: Tumor Node Metastases. cPET: conventional PET. dPET: digital PET. SUV: Standardized Uptake Value. FDG: Fluor-18 Fluordeoxyglucose